RESEARCH ARTICLE

# Water-Quality Thresholds and Formation-Damage Mechanisms during Water Injection in the Southern Area of the Deep Reservoir in the Gaoshangpu Oilfield

**Mei Luo**[1], **Qirong Qin**[1], **Shilin Wang**[1,*], **Liao Pan**[1] **and Hening Li**[1]

[1] School of Geoscience and Technology, Southwest Petroleum University, Chengdu 610500, China

## Abstract

**Injected water quality critically determines waterflooding effectiveness. The southern area of Gaoshen, a major deep reservoir block of the Gaoshangpu Oilfield (Jidong Oilfield), faces severe injection-well plugging, increased injection pressure, failing injection rates, and rapid production decline—necessitating urgent water-quality optimization. This study conducts reservoir sensitivity evaluation, injected water–reservoir compatibility analysis, and single-factor experiments on the effects of solid particles, suspended oil, and bacteria on permeability. Results show: (1) The reservoir exhibits moderately strong water sensitivity (critical salinity: 6000–10000 mg/L); current injected-water salinity (1499.34 mg/L) is far below this threshold, which disrupts the ionic balance and causes clay swelling—one of two dominant, co-occurring damage mechanisms alongside solid-particle plugging. (2) Suspended-particle median diameter (8.145 $\mu$m) far exceeds the recommended limit ($\leq$3 $\mu$m). For this low-porosity, low-permeability reservoir (average permeability: 28.9–39.4$\times10^{-3}$ $\mu m^2$; pore-throat radius typically <5 $\mu$m), coarse particles form bridging plugs. Unfiltered water causes 47.84% permeability damage, reduced to 27.22% after fine filtration. (3) To keep damage within 20%, thresholds are: particle diameter $\leq$ 1.5 $\mu$m, concentration $\leq$ 2 mg/L, oil content $\leq$ 6 mg/L, and sulfate-reducing bacteria at 0 cells/mL. (4) Site-specific water-quality criteria are established; verification experiments show damage reduced to 17%. These findings provide a scientific basis for adjusting waterflooding plans in this area and reference for optimizing water quality in analogous reservoirs.**

**Keywords**: Gaoshangpu oilfield, low-porosity and low-permeability reservoir, water injection development, water quality optimization, formation damage.

## 1 Introduction

Water injection is the primary method for supplementing reservoir energy, and the quality of injected water is a critical factor determining the effectiveness of reservoir development [1–3], with

**Submitted:** 24 April 2026
**Accepted:** 20 June 2026
**Published:** 01 July 2026

**Vol.** 2, **No.** 3, 2026.
10.62762/JGEE.2026.411772

***Corresponding author:**
✉ Shilin Wang
ybybwsl@163.com

**Citation**
Luo, M., Qin, Q., Wang, S., Pan, L., & Li, H. (2026). Water-Quality Thresholds and Formation-Damage Mechanisms during Water Injection in the Southern Area of the Deep Reservoir in the Gaoshangpu Oilfield. *Journal of Geo-Energy and Environment*, 2(3), 230–243.

formation damage arising from mechanisms such as scale deposition [4, 5] and oily-water injection [6]. This issue remains a major focus of waterflooding operations across diverse reservoir types, from offshore fields [7] to ultra-low-permeability [8–10] and tight sandy-conglomerate reservoirs [11, 12]. Beyond traditional experimental approaches, data-driven methods have been applied to predict water-quality impacts on sandstone reservoir permeability [13]; however, such approaches typically require large field datasets and lack the mechanistic interpretability necessary for site-specific threshold determination, which is the primary objective of the present study. Solid particles, suspended oil, bacteria, and incompatible chemical components in the injected water can all cause a decline in reservoir permeability, leading to increased injection pressure, failure to meet the required injection rates, insufficient reservoir energy replenishment, and ultimately a reduction in oil recovery [2, 8].

Considerable research has been conducted on the mechanisms and evaluation methods of formation damage caused by water quality. Regarding the mechanisms of solid particle damage, Barkman and Davidson [14] introduced the concept of "water quality ratio" for calculating formation damage rate. Abrams [15], Oort et al. [16], and Eylander [17] all indicated that the ratio of suspended particle diameter to pore-throat diameter is key in determining plugging. The widely accepted "1/3–1/2 bridging rule" suggests that bridging plugging occurs when the particle diameter exceeds one-third to one-half of the pore-throat diameter. For low-permeability reservoirs, the optimal particle diameter is approximately 0.5–2 $\mu$m. In terms of damage mechanisms and evaluation methods, Wojtanowicz et al. [18], Rochon et al. [19], and Pang and Sharma [20] contributed quantitative models for particle invasion, damage stage division (from internal damage to external filter cake formation), and the exponential relationship between permeability reduction and particle concentration/flow rate, respectively. Regarding multi-factor water quality effects, Sharma et al. [21] and Bansal & Caudle [22] emphasized the need for comprehensive assessment of water chemistry, bacteria, suspended solids, oil content, and clay properties, noting that even using "perfect" water, reservoir heterogeneity may still cause injection difficulties. Bennion et al. [23] further demonstrated that formation damage mechanisms are inherently multi-factorial, with clay mineralogy, fluid incompatibility, and particulate invasion acting in combination to impair permeability across diverse reservoir types. Furthermore, Al-Taq et al. [24] identified sulfate scale as a major source of water injection problems, while Karazincir et al. [25] found that filter cake permeability formed by oil-wet solids is 10%–50% lower than that formed by oil-free particles. Field investigations have further documented the practical consequences of these damage mechanisms: clay swelling-induced permeability impairment has been reported as a primary cause of injection pressure buildup in low-permeability formations in the Changqing Oilfield [26], while Dong et al. [27] demonstrated a direct correlation between pipeline corrosion and progressive deterioration of injected water quality in low-permeability oilfield systems. In the context of water quality standards for low-permeability reservoirs, Xiong et al. [2] proposed effective water quality limits, and Rossini et al. [7] optimized injection water quality indicators for an offshore S oilfield through laboratory simulation.

However, the above studies also reveal a key issue: due to differences in reservoir physical properties, mineral composition, and fluid characteristics among oilfields, water quality indicators are highly site-specific and difficult to apply directly. The Gaoshangpu Oilfield is located in the Nanpu Sag of the Bohai Bay Basin and is characterized by heterogeneous reservoir properties, as well as high wax, resin, and asphaltene content in the crude oil. The southern area of Gaoshangpu Shen (hereinafter referred to as 'the southern area of Gaoshen') generally exhibits low porosity, low permeability, and strong heterogeneity. Current development conditions indicate that although long-term water injection has led to the formation of many large channels, some injection wells still experience plugging. This results in increased injection pressure, failure to meet the required injection rates, insufficient reservoir energy replenishment, accelerated production decline, and continuously diminishing waterflooding effectiveness. The causes may include incompatibility between the injected water and the reservoir rock, solid particle plugging, organic precipitation, and bacterial proliferation. To date, however, no systematic experimental study has been conducted to identify the dominant formation damage mechanisms or to establish quantitative water quality thresholds for this specific reservoir. Specifically, the main controlling factors of formation damage in this area remain unclear, the quantitative thresholds for various water

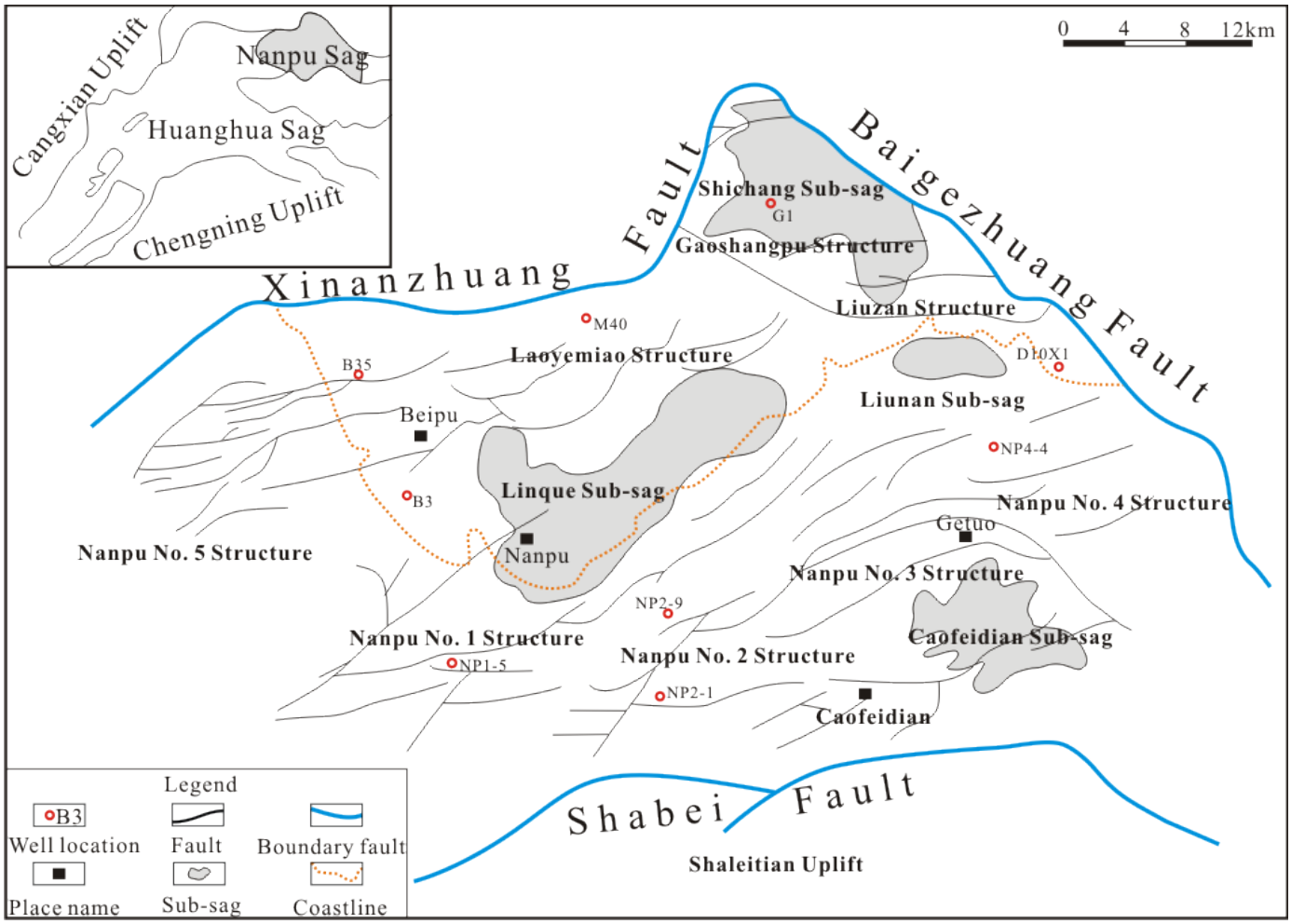


**Figure 1.** Geological Structural Map of the southern area of Gaoshen.

quality indicators (solid particle size, solid particle concentration, oil content, bacterial concentration, salinity) have not been established, and there is no experimental basis for whether and how the existing water quality indicators need to be adjusted.

To address this gap, the present study, based on laboratory experiments targeting the reservoir characteristics and current injected water quality of the southern area of Gaoshen, aims to: (1) identify and evaluate the main controlling factors of reservoir permeability damage and their mechanisms; (2) quantitatively determine the reasonable thresholds for key water quality indicators such as solid particle size, solid particle concentration, oil content, and bacterial concentration; (3) establish site-specific injection-water quality criteria for the low-porosity, low-permeability reservoir in this area. The findings provide a scientific basis for adjusting the waterflooding development plan in this area and may serve as a useful reference for optimizing water quality in reservoirs with similar permeability, clay mineral composition, and pore-throat structure.

## 2 Geological Background

The Gaoshangpu Oilfield is located in the Gaoshangpu structural belt in the northern part of the Nanpu Sag, within the Huanghua Depression, northern Bohai Bay Basin. The Gaoshangpu area is adjacent to two source sub-sags: to the north is the Shichang source sub-sag controlled by the Baigezhuang Fault, and to the southwest is the Linque source sub-sag controlled by the Gaoliu and Xinanhuangzhuang Faults (Figure 1). The $Es_3^{4+5}$ mudstone in the northern sub-sag is the main source rock, while the $Es_1$, $Ed_2$, and upper $Ed_3$ sub-members in the southwestern sub-sag are fair to good source rocks. Three types of hydrocarbon migration pathways exist in this area: faults, sand bodies, and unconformities, with faults being the primary pathway. Overall, the development of middle-deep oil layers in this area is controlled by both structure and lithology, exhibiting significant lateral variation, dominated by lithologic or structural-lithologic reservoirs [28].

The main oil-bearing intervals in the southern area

of Gaoshen are the $Es_3^{2+3}$ II and III oil groups. The reservoir physical properties vary considerably, with extremely strong heterogeneity. The permeability of the II oil group ranges from 2.4 to $159.0\times10^{-3}$ $\mu m^2$, averaging $39.4\times10^{-3}$ $\mu m^2$, with a permeability differential of 66.3. The permeability of the III oil group ranges from 2.2 to $116.2\times10^{-3}$ $\mu m^2$, averaging $28.9\times10^{-3}$ $\mu m^2$, with a permeability differential of 19.8. Overall, this represents a low-porosity, low-permeability reservoir.

Regarding clay mineral composition (Table 1), the $Es_3^{2+3}$ II oil group has relatively low kaolinite content, while the III oil group has higher kaolinite content (15%–39%), indicating some potential for velocity sensitivity. Both oil groups have relatively high contents of montmorillonite or illite-smectite mixed layers, exhibiting moderate to strong water sensitivity. This feature is a key basis for the subsequent experimental design of water sensitivity evaluation—the high content of montmorillonite and illite-smectite mixed layers means that the reservoir in this area is highly sensitive to changes in injected water salinity, and low-salinity water injection may induce significant clay hydration swelling.

Furthermore, the reservoir crude oil has low viscosity but high wax, resin, and asphaltene content, making it prone to forming organic precipitates that can cause formation plugging when formation temperature and pressure drop. The formation water is primarily of the $NaHCO_3$ type (Table 2), with low total salinity, typically ranging from 2700 to 5000 mg/L. It has high $HCO_3^-$ content and certain amounts of $SO_4^{2-}$, $Ca^{2+}$, and $Mg^{2+}$, indicating scaling potential—an issue that requires attention in subsequent compatibility experiments.

## 3 Samples and Methods

### 3.1 Sample Collection and Current Water Quality Determination

Samples for this study were taken from the southern area of Gaoshen, mainly including:

(1) Core samples: A total of 62 core plugs were selected from the main pay zones ($Es_3^{2+3}$ II & III) in the southern area of Gaoshen. After cleaning and drying, the measured gas permeability ranged from $11.566\times10^{-3}$ to $97.169\times10^{-3}$ $\mu m^2$, and porosity ranged from 14.17% to 14.80%, characteristic of a low-porosity, low-permeability reservoir. Core plugs were grouped according to experimental objectives: 12 plugs for solid particle size experiments (gas permeability 23.66–$50.30\times10^{-3}$ $\mu m^2$), 9 plugs for solid particle concentration experiments (permeability 19.02–$46.70\times10^{-3}$ $\mu m^2$), 18 plugs for suspended oil experiments (gas permeability 14.51–$45.43\times10^{-3}$ $\mu m^2$), 11 plugs for bacteria experiments (permeability 16.69–$97.17\times10^{-3}$ $\mu m^2$), 3 plugs for water sensitivity evaluation, and 2 plugs for compatibility verification.

(2) Injected water samples: Collected from the outlet of the water injection station in the southern area of Gaoshen. Before sampling, the valve was opened to allow flow at 5–6 L/min for 3 minutes to ensure sample representativeness.

(3) Formation water samples: Collected from representative production wells (Gao 13, Gao 62-30, Gao 88) in the southern area of Gaoshen for compatibility experiments.

(4) Crude oil samples: Collected from production wells in the southern area of Gaoshen for compatibility analysis with injected water.

### 3.2 Injected Water Quality Analysis Methods

Based on industry standards SY/T 5329-2022 [29] "Recommended indicators and analysis methods for water injection quality in clastic reservoirs" and SY/T 5523-2025 [30] "Analysis methods for oilfield water", the following parameters of the injected water samples were determined:

(1) Suspended solid content: Determined via membrane filtration using cellulose ester membranes with an average pore size of 0.45 $\mu m$. After vacuum filtration, the membrane was dried to constant weight,

**Table 1.** Clay mineral analysis data of the southern area of Gaoshen.

| Well number | Well section (m) | Relative clay mineral content/% | | | | | |
|---|---|---|---|---|---|---|---|
| | | Montmorillonite | Illite | Illite-smectite mixed layers | Kaolinite | Chlorite | Mix ratio |
| G103-4 | 3513.31–3590.97 | 20–75 | 3–14 | 6–64 | 8–16 | 9–87 | 71.20 |
| G15-20 | 3478.82–3520.28 | 3–35 | 28–62 | 2–6 | / | 19–72 | 18.75 |
| G102-4 | 3518.50–3574.30 | / | 1–13 | 11–45 | 15–39 | 17–64 | 46.17 |

**Table 2.** Ion statistics of the original formation water of the southern area of Gaoshen (mg/L).

| Fault block | $Na^+$+$K^+$ | $Ca^{2+}$ | $Mg^{2+}$ | $SO_4^{2-}$ | $HCO_3^-$ | $CO_3^{2-}$ | $Cl^-$ | Water type | Salinity (mg/L) |
|---|---|---|---|---|---|---|---|---|---|
| Gao 13 | 1503 | 64 | 36 | 196 | 1030 | 2 | 1834 | $NaHCO_3$ | 4664 |
| Gao 62-30 | 633 | 25 | 7 | 259 | 1151 | 0 | 179 | $NaHCO_3$ | 2254 |
| Gao 88 | 1449 | 35 | 16 | 270 | 1023 | 0 | 1547 | $NaHCO_3$ | 4340 |
| Average | 1195 | 41 | 20 | 242 | 1068 | 1 | 1187 | $NaHCO_3$ | 3754 |

and the suspended solid content was calculated based on the membrane weight gain and the volume of water filtered.

(2) Median diameter of suspended particles: Determined using a microscopic particle analyzer. The median diameter corresponds to the particle diameter at which the cumulative particle volume accounts for 50% of the total particle volume.

(3) Oil content: Under acidic conditions, petroleum ether was used to extract petroleum substances from the water, and the oil content was determined by gravimetric analysis.

(4) Bacterial content: Sulfate-Reducing Bacteria (SRB), Total General Bacteria (TGB), and Iron Bacteria (IB) were determined using the MPN (Most Probable Number) method. After on-site inoculation, samples were incubated at reservoir temperature (90 °C). Bacterial content was calculated based on bacterial growth.

(5) Ion content: Cation concentrations ($Ca^{2+}$, $Mg^{2+}$) were determined by atomic absorption spectrometry. Anion concentrations ($HCO_3^-$, $CO_3^{2-}$, $SO_4^{2-}$) were determined by titration.

(6) Total iron content: Determined using the 1,10-phenanthroline spectrophotometric method.

### 3.3 Reservoir Rock Sensitivity Evaluation Method

Reservoir water sensitivity was evaluated according to SY/T 5358 "Experimental evaluation method for sandstone reservoir sensitivity". The specific steps are as follows:

(1) Critical salinity determination: Brines with different salinities were prepared (salinity gradient: original formation water salinity, 20000 mg/L, 15000 mg/L, 10000 mg/L, 8000 mg/L, 6000 mg/L, 4000 mg/L, 2000 mg/L, distilled water). The brine was injected sequentially from high to low salinity through the core. The permeability at each salinity was measured, and a curve of permeability vs. salinity was plotted. The salinity at which permeability began to significantly decrease was taken as the critical salinity.

(2) Water sensitivity index calculation: Calculated according to the following formula:

$$I_w = \frac{K_i - K_w}{K_i}$$

where $I_w$ = water sensitivity index, %; $K_i$ = initial permeability, $10^{-3}$ $\mu m^2$; $K_w$ = permeability after distilled water flooding, $10^{-3}$ $\mu m^2$.

Classification standard for water sensitivity degree: $I_w \leq 0.30$ (weak), $0.30 < I_w \leq 0.50$ (moderately weak), $0.50 < I_w \leq 0.70$ (moderately strong), $I_w > 0.70$ (strong).

### 3.4 Evaluation Method for Injected Water-Reservoir Compatibility

(1) Compatibility evaluation of injected water and formation water: Finely filtered injected water (filtered through 0.45 $\mu$m membrane to remove solid particles and bacteria) was mixed with formation water in a 1:1 ratio. The mixture was injected into artificial cores (with permeability similar to reservoir rock) at a constant rate. The change in core permeability during the injection of 100 pore volumes (PV) was measured, and the permeability damage rate was calculated to evaluate the degree of formation damage caused by scaling. The experiment was conducted at 90 °C with a confining pressure of 3.5 MPa. Artificial cores were used for this experiment because the limited availability of natural cores with matched permeability precluded their use for long-duration (100 PV) compatibility flooding; however, this substitution may affect the representativeness of scaling results relative to the natural reservoir, which is acknowledged as a limitation.

(2) Compatibility evaluation of injected water and reservoir crude oil: Two methods were used: Method 1 (Membrane filtration method): Equal volumes of crude oil and injected water were mixed in a glass bottle, shaken, and placed in a 90 °C water bath for 2 hours, then cooled to room temperature. The mixture was filtered through a 100-mesh screen, and

the residue on the screen was washed with refined oil. If the residue was solid, it indicated a tendency for sludge formation; if liquid, it indicated emulsion formation.

Method 2 (Microscopic observation method): A drop of crude oil was placed on a glass slide, a small amount of injected water was added, a cover slip was applied, and the edge of the oil droplet was observed under a microscope. If a visible, firm film formed around the oil droplet, it indicated a tendency for sludge formation.

(3) Compatibility evaluation of injected water and reservoir rock: Reservoir cores were cleaned, dried, crushed, and sieved through a 100-mesh screen. Equal amounts of core powder were placed into graduated cylinders with stoppers, and the dry volume was recorded. Formation water and injected water were added to respective cylinders to the same mark. The cylinders were shaken thoroughly and allowed to stand statically at 90 °C for 24 hours to allow the core powder to fully swell. The final volumes of core powder in formation water ($V_1$) and injected water ($V_2$) were measured and recorded. If $V_2 > V_1$, it indicated that the injected water caused clay swelling; if $V_2 \leq V_1$, it indicated that the injected water did not cause clay swelling.

### 3.5 Volumetric Flow-Through Experiment Method

The volumetric flow-through experiment was used to evaluate the impact of injected water quality on reservoir permeability and is the core experimental method for determining water quality indicators. The experimental steps are as follows:

(1) Core preparation: Natural cores were cleaned, dried, and their gas permeability and porosity were measured. After vacuum saturation with formation water, the liquid permeability was measured as the initial permeability ($K_i$).

(2) Experimental fluid preparation: Injected water with different quality indicators was prepared according to the experimental objectives. The gradient selection for each indicator in the single-factor experiments was based on the following considerations: the solid particle size gradient (1, 1.26, 1.5, 1.6, 2 $\mu$m) covered the range from below to above the industry-recommended value ($\leq 3$ $\mu$m) to determine the sensitivity threshold of the reservoir to particle size; the solid particle concentration gradient (1, 2, 3 mg/L) was appropriately extended based on the field-measured value (2.5 mg/L); the oil content gradient (6, 8, 10, 15 mg/L) was set with gradients slightly below and above the standard requirement of $\leq$ 8 mg/L for low-permeability reservoirs in SY/T 5329-2012; the SRB concentration gradient (0, 25, 50 cells/mL) was set according to the standard requirement of $\leq 25$ cells/mL, with both compliant and non-compliant conditions. Solid particles were obtained by grinding and sieving reservoir cuttings. Suspended oil was prepared by emulsifying and dispersing field crude oil.

(3) Displacement experiment: The core was mounted in a core holder, with a confining pressure of 3.5 MPa and temperature of 90 °C. The prepared injected water was injected into the core at a constant rate (0.5–1.0 mL/min). Displacement pressures at different injected pore volumes (10 PV, 20 PV, 30 PV, 40 PV, 50 PV, 60 PV, 100 PV) were recorded. Permeability ($K$) at each stage was calculated using Darcy's law.

(4) Permeability damage rate calculation:

$$D = \frac{K_i - K}{K_i} \times 100\%$$

where $D$ = permeability damage rate, (%), $K_i$ = initial permeability, ($10^{-3}$ $\mu$m$^2$), $K$ = permeability after injecting a certain volume, ($10^{-3}$ $\mu$m$^2$).

(5) Experimental grouping design: Solid particle size effect experiment (fixed concentration 2 mg/L, diameter gradient: 1, 1.26, 1.5, 1.6, 2 $\mu$m); Solid particle concentration effect experiment (fixed diameter 1.5 $\mu$m, concentration gradient: 1, 2, 3 mg/L); Suspended oil effect experiment (oil content gradient: 6, 8, 10, 15 mg/L); Bacteria effect experiment (SRB content gradient: 0, 25, 50 cells/mL).

(6) Optimization target determination: A permeability damage rate of less than 20% after injecting 50 PV was set as the target for water quality indicator optimization. This target was established based on the following considerations: first, referencing the "acceptable" damage range in industry standards; second, considering field economic feasibility, as overly stringent indicators would significantly increase water treatment costs; third, the verification experiments in this study demonstrate that this target is achievable.

### 3.6 Experimental Equipment

Main experimental equipment includes: Core displacement apparatus (with constant-rate constant-pressure pump, core holder, confining pressure pump, pressure sensors, oven); Water quality

**Table 3.** Injected water analysis data in the southern area of Gaoshen.

| Cation content (mg/L) | | Anion content (mg/L) | | Total salinity (mg/L) | Total hardness (mg/L) | pH value |
|---|---|---|---|---|---|---|
| $K^+$ | 9.33 | $Cl^-$ | 295.00 | | | |
| $Na^+$ | 405.20 | $SO_4^{2-}$ | 12.00 | | | |
| $Ca^{2+}$ | 17.31 | $HCO_3^-$ | 747.00 | 1499.34 | 96.75 | 7.70 |
| $Mg^{2+}$ | 13.00 | $CO_3^{2-}$ | 0.00 | | | |
| **Total** | **444.84** | **Total** | **1054.50** | | | |

analysis equipment (microporous membrane filtration tester, electronic balance, constant-temperature drying oven, microscope and image analysis system, atomic absorption spectrophotometer); Bacterial culture equipment (sterile workbench, constant-temperature incubator, MPN method bacterial test bottles).

## 4 Results

### 4.1 Current Injected Water Quality

The water quality indicators of the outlet water sample from the southern area of Gaoshen injection station were measured, and the results are shown in Tables 3 and 4. The median diameter of suspended solid particles in the water sample was 8.145 $\mu$m, far exceeding the requirement for low-permeability reservoirs in standard SY/T 5329-2012 (typically $\leq$ 3 $\mu$m). Total iron content was 10.0 mg/L, oil content was 0.83 mg/L, and suspended solid content was 2.5 mg/L. Bacteria (SRB, TGB, Iron bacteria) were not detected.

**Table 4.** Water quality analysis data of injected water in the southern area of Gaoshen.

| Index | Content |
|---|---|
| Total iron content (mg/L) | 10.0 |
| Oil content (mg/L) | 0.83 |
| Suspended solids content (mg/L) | 2.5 |
| Median particle diameter ($\mu$m) | 8.145 |
| SRB (cells/mL) | 0 |
| TGB (cells/mL) | 0 |
| Iron bacteria (cells/mL) | 0 |

A comparison of Tables 2 and 3 shows that the injected water salinity (1499.34 mg/L) is much lower than the average formation water salinity (3754 mg/L) and the critical salinity (6000–10000 mg/L), indicating that low-salinity water injection may induce clay swelling.

### 4.2 Compatibility Evaluation Results

(1) Compatibility with formation water: Finely filtered injected water and formation water (1:1 ratio) were injected into an artificial core. Permeability change after 100 PV injection was measured. Results showed an initial core permeability of $7.453\times10^{-3}$ $\mu$m$^2$, decreasing to $6.907\times10^{-3}$ $\mu$m$^2$ after 100 PV injection, with a permeability damage rate of only 7.3%. This indicates that the inorganic scale formed by mixing injected water and formation water has a relatively minor direct impact on reservoir permeability.

(2) Compatibility with reservoir crude oil: The compatibility between injected water and crude oil was evaluated using membrane filtration and microscopic observation. Both methods showed: no solid material generation after mixing, no firm film formation around oil droplets, and no tendency for sludge formation. This indicates that organic precipitation and emulsion plugging are not major factors in formation damage in this area.

(3) Compatibility with reservoir rock: Core powder swelling experiment results showed that the volume of the same mass of core powder in injected water was larger than that in formation water, indicating that the injected water caused hydration swelling of clay minerals.

Further sequential injection of brines with different salinities determined the critical salinity and water sensitivity index (Table 5). Results indicate that the critical salinity for the southern area of Gaoshen reservoir rock is 6000–10000 mg/L, with water sensitivity indices ranging from 0.52 to 0.69, indicating moderately strong water sensitivity. This finding is consistent with the reservoir characterization of higher montmorillonite or illite-smectite mixed layer content. The current injected water salinity (1499.34 mg/L) is significantly lower than the critical salinity, which is the fundamental cause of clay hydration swelling.

### 4.3 Water Quality Adaptability Evaluation

Volumetric flow-through experiments were used to compare the permeability damage caused by unfiltered injected water and injected water finely filtered

**Table 5.** Experimental evaluation results of water sensitivity in the southern area of Gaoshen.

| Core No. | Well depth (m) | Air permeability ($10^{-3}$ $\mu m^2$) | Porosity (%) | Critical salinity (mg/L) | Water sensitivity index | Water sensitivity degree |
|---|---|---|---|---|---|---|
| G102-4-5-1 | 3564.98 | 11.937 | 14.29 | 10000 | 0.52 | Moderately strong |
| G62-35-6-3 | 3831.90 | 11.786 | 14.80 | 8000 | 0.69 | Moderately strong |
| G93-11-4 | 3510.96 | 11.566 | 14.17 | 6000 | 0.55 | Moderately strong |

through a 0.45 $\mu$m membrane (Figure 2). Results showed that the permeability damage rate caused by unfiltered injected water was 47.84%, while that caused by finely filtered injected water was 27.22%. The difference between the two is 20.62 percentage points, which can be attributed to the contribution of solid particle plugging. The 27.22% damage rate that still exists even after fine filtration is mainly attributed to clay hydration swelling.

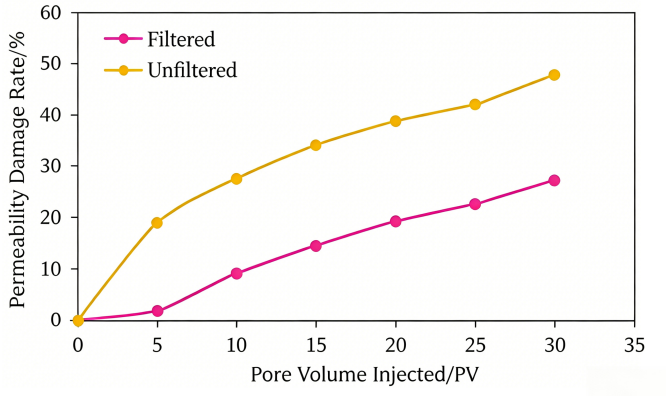


**Figure 2.** Comparison of permeability damage caused by filtered and unfiltered injected water.

### 4.4 Effect of Water Quality Indicators on Permeability

#### *4.4.1 Effect of Solid Particle Size*

Using 12 core plugs, injected water with a fixed solid particle concentration of 2 mg/L but varying mean diameters (1, 1.26, 1.5, 1.6, 2 $\mu$m) was prepared for volumetric flow-through experiments (injection of 50 PV). Results (Figures 3 and 4) showed that as the solid particle diameter in the injected water increased, the permeability damage increased rapidly; the overall damage rate decreased with increasing core permeability. To achieve permeability damage less than 20% under a solid particle concentration not exceeding 2 mg/L, the solid particle diameter should be controlled at $\leq$ 1.5 $\mu$m.

#### *4.4.2 Effect of Solid Particle Concentration*

Injected water with a fixed particle diameter of 1.5 $\mu$m and concentrations of 1, 2, and 3 mg/L

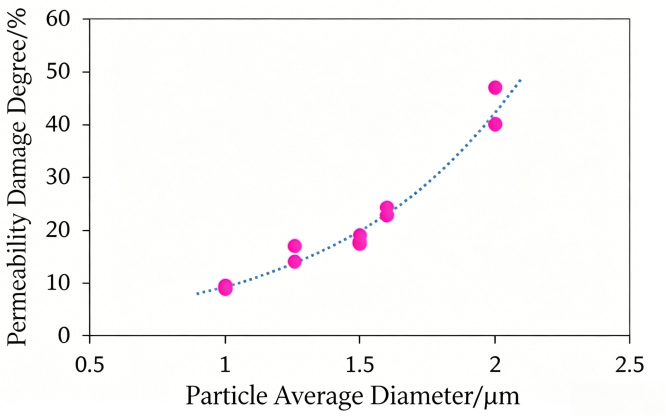


**Figure 3.** Relationship between particle diameter and permeability damage in injected water.

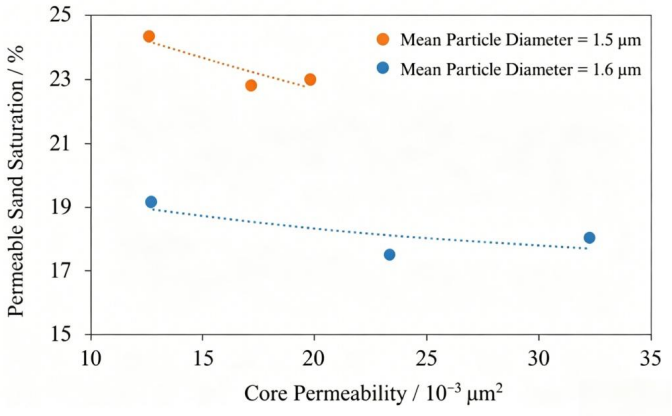


**Figure 4.** Relation curve between damage rate of solid particles and core permeability.

was prepared. Using 9 core plugs, volumetric flow-through experiments were conducted. Results (Figures 5 and 6) showed that under different particle concentrations, the permeability damage rate increased with the volume of injected water and decreased with increasing core permeability. Under cumulative injection of 50 PV, the permeability damage rate was 10.28%–11.58% at a particle concentration of 1 mg/L, 12.98%–14.68% at 2 mg/L, but sharply rose to over 45% at 3 mg/L. For a solid particle diameter of 1.5 $\mu$m and target permeability damage rate $<$ 20%, the solid particle concentration in the injected water should be controlled at $\leq$ 2 mg/L.

**Table 6.** Experimental results of the influence of bacterial content on reservoir permeability.

| Core sample No. | Permeability ($10^{-3}$ $\mu m^2$) | | Bacterial content (cells/mL) | Permeability retention rate under different pore volume (PV) injection multiples (%) | | | | | | |
|---|---|---|---|---|---|---|---|---|---|---|
| | Air-measured | Initial | | 10 | 20 | 30 | 40 | 50 | 60 | 100 |
| G66-32-2-3-2 | 30.579 | 16.83 | 0 | 100 | 100 | 100 | 100 | 99 | 98 | 97 |
| G93-7-1-1 | 94.942 | 63.29 | 0 | 100 | 100 | 100 | 100 | 99 | 99 | 96 |
| G102-4-8-7-2 | 19.912 | 9.52 | 25 | 100 | 100 | 100 | 100 | 98 | 98 | 96 |
| G102-4-d4 | 32.04 | 15.96 | 25 | 100 | 100 | 100 | 100 | 99 | 98 | 98 |
| G102-4-d1 | 40.241 | 18.34 | 25 | 100 | 100 | 100 | 100 | 98 | 98 | 97 |
| G102-4-d2 | 41.549 | 20.44 | 25 | 100 | 100 | 100 | 100 | 98 | 97 | 97 |
| G102-4-d3 | 45.323 | 23.27 | 25 | 100 | 100 | 100 | 100 | 99 | 98 | 97 |
| G93-7-1-2 | 97.169 | 65.21 | 25 | 100 | 100 | 100 | 100 | 99 | 98 | 97 |
| G66-32-3-2 | 16.685 | 5.8 | 50 | 100 | 100 | 100 | 100 | 98 | 97 | 96 |
| G66-32-d2 | 26.504 | 12.98 | 50 | 100 | 100 | 100 | 100 | 99 | 98 | 96 |
| G66-32-d1 | 30.544 | 14.59 | 50 | 100 | 100 | 100 | 100 | 98 | 98 | 97 |

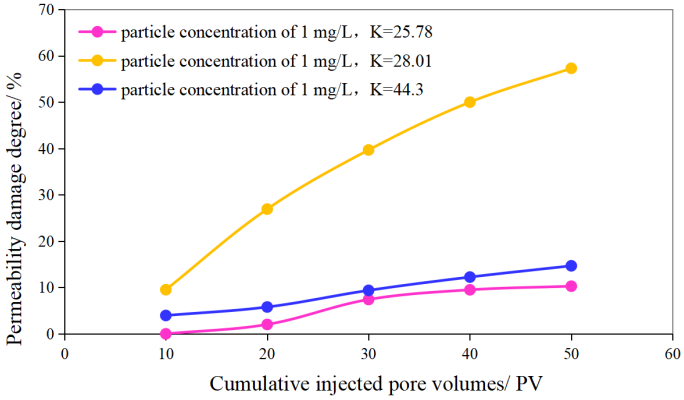


**Figure 5.** Variation curve of permeability damage rate under different injected water volumes.

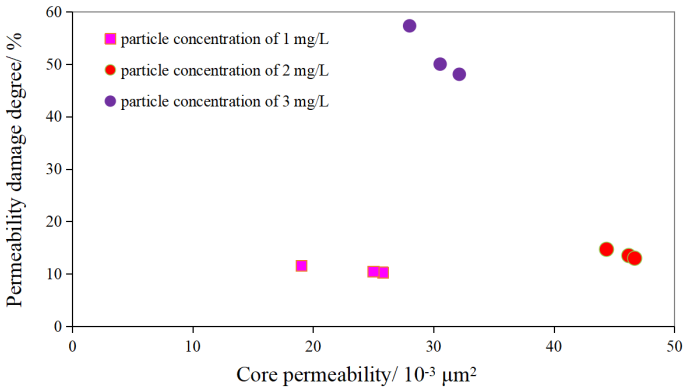


**Figure 6.** Relationship between damage rate of solid particle concentration and core permeability.

### 4.4.3 *Effect of Suspended Oil*

Injected water with oil contents of 6, 8, 10, and 15 mg/L was prepared. Using 18 core plugs, volumetric flow-through experiments were conducted. Results (Figures 7 and 8) showed that for a given oil content, the damage rate did not decrease significantly with increasing core permeability, indicating that cores with different permeabilities are sensitive to suspended oil. As the oil content in the injected water increased, core permeability significantly decreased. The oil content should be controlled within 6 mg/L to ensure the permeability damage rate is less than 20%.

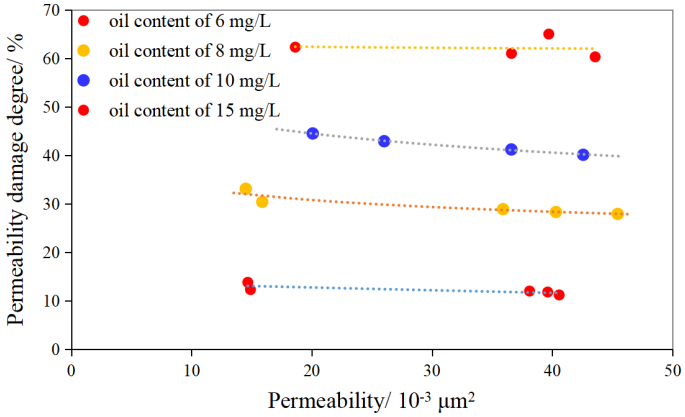


**Figure 7.** Variation curve of core damage rate with permeability under different oil content.

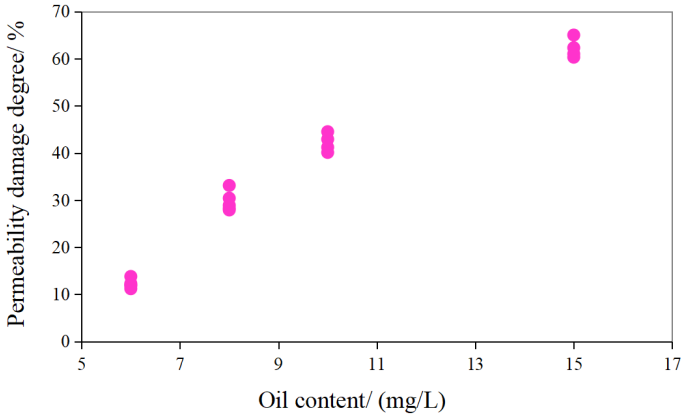


**Figure 8.** Relation curve between oil content in injected water and permeability damage rate.

#### 4.4.4 *Effect of Bacteria*

Injected water with SRB concentrations of 0, 25, and 50 cells/mL was prepared. Using 11 core samples, permeability was measured after injecting different water volumes. Experimental results (Table 6) showed that even when the bacterial concentration reached 50 cells/mL, after injecting 100 PV of bacteria-laden water, the permeability retention rate remained at or above 96%, similar to results with 0 cells/mL. This indicates that in short-term core displacement experiments, SRB themselves have a limited direct impact on permeability. However, this does not mean that control over SRB can be relaxed: given its potential to induce corrosion, sulfide precipitation, reservoir souring, and long-term injection system risks, SRB should still be strictly controlled.

### 4.5 Water Quality Indicator Optimization and Verification

Based on the comprehensive results of the single-factor experiments, and targeting a permeability damage rate $< 20\%$ at an injected pore volume of 50 PV, the optimized injected water quality indicator system for the southern area of Gaoshen is as follows:

- **Suspended Solid Content**: $< 2$ mg/L
- **Median Suspended Particle Diameter**: $< 1.5\,\mu$m
- **Oil Content**: $< 6$ mg/L
- **Sulfate-Reducing Bacteria (SRB)**: 0 cells/mL
- **Salinity**: Not lower than formation water salinity ($> 6000$ mg/L)

**Table 7.** Core flow-through experimental results under the optimized injection-water quality criteria.

| Index | Core sample No. | |
|---|---|---|
| | G102-4-8-1 | G102-4-8-2 |
| Air-measured permeability ($10^{-3}\,\mu m^2$) | 48.351 | 49.706 |
| Initial permeability ($10^{-3}\,\mu m^2$) | 26.266 | 29.585 |
| Particle concentration (mg/L) | 2 | 2 |
| Particle diameter ($\mu$m) | 1.5 | 1.5 |
| Mean particle content (mg/L) | 6 | 6 |
| Oil content (mg/L) | 0 | 0 |
| Bacterial content (cells/mL) | 0 | 0 |
| Permeability damage rate at 10 PV (%) | 0 | 0 |
| Permeability damage rate at 20 PV (%) | 6.02 | 5.88 |
| Permeability damage rate at 30 PV (%) | 11.09 | 13.11 |
| Permeability damage rate at 40 PV (%) | 16.96 | 16.11 |
| Permeability damage rate at 50 PV (%) | – | 17.11 |

According to the new water quality indicators, injected water was prepared. Two core plugs not used in previous experiments (G102-4-8-1 and G102-4-8-2) were selected for volumetric flow-through experiments. The results (Table 7) showed that core G102-4-8-2 achieved a permeability damage rate of 17.11% at 50 PV, meeting the optimization target of less than 20%. Core G102-4-8-1 reached 16.96% damage at 40 PV before the experiment was terminated; extrapolation of its damage trend (6.02% at 20 PV, 11.09% at 30 PV, 16.96% at 40 PV) suggests it would also remain below the 20% threshold at 50 PV, consistent with the result from G102-4-8-2.

## 5 Discussion

### 5.1 Main Controlling Factors of Formation Damage and Their Mechanisms

Based on the comprehensive experimental results above, the main controlling factors for formation damage during water injection in the southern area of Gaoshen can be summarized into two mutually reinforcing mechanisms.

(1) Clay hydration swelling is a fundamental factor causing formation damage in this area. The southern area of Gaoshen has relatively high contents of montmorillonite and illite-smectite mixed layers (Table 1), resulting in water sensitivity indices of 0.52–0.69, indicating moderately strong water sensitivity. The current injected water salinity (1499.34 mg/L) is significantly lower than the reservoir's critical salinity (6000–10000 mg/L). Injection of this low-salinity water disrupts the ionic balance between the formation water and clay minerals, leading to cation exchange in the interlayers of clay minerals and water molecule entry, causing lattice expansion. The volume of swollen clay minerals can increase several to tens of times their original size. After dispersion and migration, they cause plugging at pore throats, resulting in irreversible permeability decline. This mechanism was fully verified in the volumetric flow-through experiments: even with fine filtration (excluding solid particle effects), the injected water still caused a 27.22% permeability damage, primarily attributable to clay swelling.

(2) Solid particle plugging is another key factor causing formation damage in this area. The median diameter of suspended solid particles in the current injected water is as high as 8.145 $\mu$m, far exceeding the recommended value for low-permeability reservoirs in industry standards ($\leq 3\,\mu$m). For the low-porosity, low-permeability reservoir with average permeability of only $28.9–39.4\times10^{-3}\,\mu m^2$, the pore-throat radius is typically less than 5 $\mu$m. According to the classic "1/3–1/2 bridging rule", when the particle diameter exceeds 1/3 to 1/2 of the pore-throat diameter, particles

**Table 8.** Comparison of optimized indicators in this study with industry standards.

| Water Quality Indicator | SY/T 5329-2012 (Low-permeability Reservoir) | Optimized Indicators in This Study | Stringency |
|---|---|---|---|
| Suspended Solid Content (mg/L) | $\leq 3$ | $< 2$ | More stringent |
| Median Suspended Particle Diameter ($\mu$m) | $\leq 3$ | $< 1.5$ | More stringent |
| Oil Content (mg/L) | $\leq 8$ | $< 6$ | More stringent |
| SRB (cells/mL) | $\leq 25$ | 0 | More stringent |

**Table 9.** Comparison of water quality indicators for similar reservoirs.

| Reservoir/Block | Permeability ($10^{-3}$ $\mu m^2$) | Suspended Solid (mg/L) | Median Particle Diameter ($\mu$m) | Oil Content (mg/L) | Source |
|---|---|---|---|---|---|
| The southern area of Gaoshen | 28.9–39.4 | $< 2$ | $< 1.5$ | $< 6$ | This study |
| Ultra-low permeability reservoir, NW China | 0.1–1.65 | $< 30$ | $< 5$ | $< 10$ | Tang et al. [8] |
| Jilin Oilfield tight reservoir | 1.0–10.0 | $< 3$ | $< 2$ | $< 8$ | Cao et al. [11]* |

* Water quality criteria cited from the operational injection standards reported in Cao et al. [11].

cannot easily pass through the pore throat and form bridges at the pore throat entrance. As the injected water volume increases, bridging accumulates to form dense "external filter cakes" and "internal filter cakes", leading to continuous permeability decline. Experimental data show that unfiltered injected water caused 47.84% permeability damage, which decreased to 27.22% after filtration, a difference of 20.62 percentage points, directly reflecting the contribution of solid particles.

Contribution of other factors: Inorganic scaling and organic precipitation have a smaller impact on formation damage in this area. Compatibility experiments between injected water and formation water showed that even at a high injection volume of 100 PV, the permeability damage rate caused by scaling was only 7.3%. Compatibility experiments with crude oil also showed no tendency for sludge or emulsion formation. As noted in the experimental results, SRB showed limited direct permeability impact in short-term tests; however, field experience from similar oilfields has demonstrated that sustained bacterial activity can lead to $H_2S$-induced corrosion, iron sulfide precipitation, and progressive reservoir souring over production timescales—risks that justify the adoption of the most stringent control standard (0 cells/mL) despite the benign short-term experimental data. Long-term impacts of SRB on reservoir permeability through biogenic $H_2S$ production and iron sulfide (FeS) precipitation have been well documented in field studies of similar waterflooding operations [27], providing the basis for adopting the most conservative control threshold (0 cells/mL) as a precautionary measure consistent with industry best practice for reservoirs sensitive to secondary mineral precipitation.

### 5.2 Comparison with Industry Standards and Similar Reservoirs

Comparing the water quality indicators optimized in this study with the current industry standard SY/T 5329-2012 (Table 8) shows that the indicators proposed in this study are more stringent.

This stricter requirement is dictated by the specific reservoir conditions of the southern area of Gaoshen: (1) The reservoir has low permeability (average 28.9–39.4$\times 10^{-3}$ $\mu m^2$) and small pore-throat radii, making it more sensitive to solid particle size; (2) The clay minerals have high contents of montmorillonite and illite-smectite mixed layers, resulting in strong water sensitivity and sensitivity to salinity changes; (3) The crude oil has high wax, resin, and asphaltene content. Although no issues were identified in the compatibility experiments, oil content still needs cautious control.

Comparing the results of this study with water quality optimization results from other low-porosity, low-permeability oilfields (Table 9) reveals a common pattern: the stringency of water quality indicators is positively correlated with reservoir permeability—the lower the permeability, the more stringent the water quality requirements. The permeability of the southern area of Gaoshen lies between that of the ultra-low permeability reservoir in NW China reported by Tang et al. [8] and the Jilin Oilfield tight reservoir, for which water injection operational standards are documented in Cao et al. [11], and its water quality indicators also fall between the two, reflecting the basic principle of "tailoring to the specific reservoir."

### 5.3 Engineering Significance of Water Quality Indicator Optimization

The water quality indicator system established in this study has direct engineering guidance significance for water injection development in the southern area of Gaoshen.

The control of suspended solid content and particle diameter is the most urgent task. The median particle diameter in the water sample from the field injection station outlet is as high as 8.145 $\mu$m, indicating that the existing water treatment process (mostly quartz sand filtration) has insufficient efficiency in removing fine particles. It is recommended to upgrade the filtration equipment, adopting fine filtration (such as cartridge filtration or membrane filtration), to control the median particle diameter below 1.5 $\mu$m.

The regulation of salinity requires attention. The current excessively low salinity of the injected water is the root cause of clay swelling. It is recommended to appropriately reinject produced formation water (salinity approximately 3754 mg/L) or supplement with high-salinity water sources to raise the injected water salinity to no less than 6000 mg/L, thereby inhibiting clay swelling. It should be noted that increasing salinity may have a synergistic effect with solid particle control, as higher salinity can promote the flocculation and settling of fine particles, improving filtration efficiency.

The control of suspended oil is relatively easy to achieve. The current oil content (0.83 mg/L) is already lower than the optimized indicator (6 mg/L), indicating that the existing oil removal process is effective and should be maintained.

Regarding bacterial control, although short-term core experiments show that SRB has a limited direct impact on permeability, considering the long-term risks of pipeline corrosion, sulfide precipitation, and reservoir souring that SRB may cause, it should still be strictly controlled at 0 cells/mL. It is recommended to regularly monitor the SRB concentration in the injected water to prevent corrosion and secondary mineral precipitation problems caused by bacterial growth.

### 5.4 Limitations and Prospects

This study has the following limitations, which warrant further in-depth investigation:

1. Insufficient simulation of dynamic damage processes: The volumetric flow-through experiments in this study employed a constant-rate injection mode. In contrast, actual water injection processes involve pressure fluctuations and intermittent injection, and the mechanisms of their impact on permeability damage remain unclear.

2. Lack of research on multi-factor synergistic effects: This study employed single-factor experiments to determine thresholds for various indicators. In actual water injection processes, factors such as solid particles, suspended oil, and low-salinity water coexist, and their synergistic effects may cause more severe damage than any single factor.

3. Need for enhanced field validation: Although the optimized water quality indicators have been validated through laboratory core experiments, long-term tracking validation in field injection wells has not yet been conducted. It is recommended to carry out field pilot tests to verify the practicality and cost-effectiveness of the indicators.

4. Economic evaluation not yet conducted: Stricter water quality indicators imply higher water treatment costs. Future research should integrate factors such as water treatment cost, injection stimulation benefit, and production increase effect to perform a comprehensive techno-economic evaluation to determine the optimal water quality indicators.

## 6 Conclusions

(1) The reservoir rock in the southern area of Gaoshen exhibits moderately strong water sensitivity, with a critical salinity range of 6000–10000 mg/L. The current injected water salinity (1499.34 mg/L) is far below the critical value. The injection of low-salinity water disrupts the ionic balance between formation water and clay minerals, leading to hydration and swelling of clay minerals, which is one of the fundamental causes of formation damage in this area.

(2) The median diameter of suspended solid particles (8.145 $\mu$m) in the current injected water substantially exceeds the industry-recommended limit, constituting another major factor causing reservoir plugging. For the low-porosity, low-permeability reservoir with a pore-throat radius typically less than 5 $\mu$m, coarse particles form bridging plugs at pore-throat entrances. The unfiltered injected water causes a permeability damage rate as high as 47.84%, which decreases to 27.22% after fine filtration.

(3) Through systematic single-factor experiments, targeting a permeability damage rate of less than 20% after injecting 50 PV, reasonable thresholds for various water quality indicators were determined: solid particle diameter $\leq 1.5\ \mu$m, solid particle concentration $\leq$ 2 mg/L, oil content $\leq$ 6 mg/L, sulfate-reducing bacteria 0 cells/mL, and salinity $\geq$ 6000 mg/L. On this basis, site-specific injection-water quality criteria suitable for the low-porosity, low-permeability reservoir in the southern area of Gaoshen were established.

(4) Preliminary verification experiments on two core plugs show that, using the optimized water quality indicators, the permeability damage rate at an injected pore volume of 50 PV can be controlled to approximately 17%, achieving the optimization target of less than 20%; one core (G102-4-8-1) reached 16.96% at 40 PV before the experiment was terminated due to equipment constraints; while the 50 PV data point was not obtained, the progressive damage trend is consistent with the result from G102-4-8-2 and suggests the threshold would likely be met. Completion of this experiment is recommended in future work. These criteria are more stringent than the industry standard SY/T 5329-2012, and broader validation across a larger core set is recommended to further confirm their applicability.

## Data Availability Statement

Data will be made available on request.

## Funding

This work was supported without any funding.

## Conflicts of Interest

The authors declare no conflicts of interest.

## AI Use Statement

The authors declare that no generative AI was used in the preparation of this manuscript.

## Ethical Approval and Consent to Participate

Not applicable.

## References

[1] Li, Y., & Zhang, J. (2023). Research on Optimization of Water Quality Index System for Low Permeability Reservoir Water Injection Development. *Chemistry and Technology of Fuels and Oils, 58*(6), 1018-1026. [CrossRef]

[2] Xiong, S., Chu, S., Zhao, G., He, Y., & Dou, J. (2015). Quality limit of effective injection water in low permeability reservoirs. *Petroleum Geology and Recovery Efficiency, 22*(3), 100-105. http://yqdzycsl.cnjournals.com/pgreen/article/abstract/20150318

[3] Bennion, D. B., Bennion, D. W., Thomas, F. B., & Bietz, R. F. (1998). Injection water quality-a key factor to successful waterflooding. *Journal of Canadian Petroleum Technology, 37*(06). [CrossRef]

[4] Moghadasi, J., Jamialahmadi, M., Müller-Steinhagen, H., & Sharif, A. (2004, February). Formation damage due to scale formation in porous media resulting from water injection. In *SPE International Conference and Exhibition on Formation Damage Control* (pp. SPE-86524). SPE. [CrossRef]

[5] Bedrikovetsky, P., Marchesin, D., Shecaira, F., Serra, A. L., Marchesin, A., Rezende, E., & Hime, G. (2001, March). Well impairment during sea/produced water flooding: treatment of laboratory data. In *SPE Latin America and Caribbean Petroleum Engineering Conference* (pp. SPE-69546). SPE. [CrossRef]

[6] Zhang, N. S., Somerville, J. M., & Todd, A. C. (1993, September). An experimental investigation of the formation damage caused by produced oily water injection. In *SPE Offshore Europe Conference and Exhibition* (pp. SPE-26702). SPE. [CrossRef]

[7] Rossini, S., Roppoli, G., Mariotti, P., Renna, S., Manotti, M., Viareggio, A., & Biassoni, L. (2020, January). Produced Water Quality impact on injection performance: predicting injectivity decline for waterflood design. In *International Petroleum Technology Conference* (p. D031S083R001). IPTC. [CrossRef]

[8] Tang, Y., Mu, T., Qin, J., Peng, R., Liu, M., & Xie, Y. (2025). The mechanism of reservoir damage by water injection in ultra-low-permeability reservoirs and optimization of water quality index. *Energies, 18*(6), 1455. [CrossRef]

[9] Zhu, J., Tang, X., Li, X., Wen, Y., Deng, Z., Rao, D., ... & Liu, C. (2024). The reservoir injury rules of water injection to an ultralow permeability reservoir: Experimental research based on core-NMR and microfluidic technology. *Energy & Fuels, 38*(16), 15131-15146. [CrossRef]

[10] Gong, Z., Zhang, L., Zhang, T., Yan, Z., Cong, S., Zhou, Z., & Kong, D. (2024). Evaluation of the compatibility between formation and injection water in ultra-low permeability reservoirs. *Processes, 12*(11), 2475. [CrossRef]

[11] Cao, J., Liu, Z., Zhang, Z., Wang, Y., & Wang, L. (2025). Analysis of Waterflooding Oil Recovery Efficiency and Influencing Factors in the Tight Oil Reservoirs of Jilin Oilfield. *Processes, 13*(5), 1490. [CrossRef]

[12] Lei, W. A. N. G., Zhang, H., Xiaodong, P. E. N. G.,

Panrong, W. A. N. G., Nan, Z. H. A. O., Shasha, C. H. U., ... & Linghui, K. O. N. G. (2019). Water-sensitive damage mechanism and the injection water source optimization of low permeability sandy conglomerate reservoirs. *Petroleum Exploration and Development, 46*(6), 1218-1230. [CrossRef]

[13] Song, X., Liu, Y., Song, Z., Wang, J., Yang, X., Li, G., & Fan, P. (2025). Machine learning prediction method for assessing water quality impacts on sandstone reservoir permeability and its application in energy development. *International Journal of Hydrogen Energy, 100*, 1046-1062. [CrossRef]

[14] Barkman, J. H., & Davidson, D. H. (1972). Measuring water quality and predicting well impairment. *Journal of Petroleum Technology, 24*(07), 865-873. [CrossRef]

[15] Abrams, A. (1977). Mud design to minimize rock impairment due to particle invasion. *Journal of petroleum technology, 29*(05), 586-592. [CrossRef]

[16] Oort, E. V., Van Velzen, J. F. G., & Leerlooijer, K. (1993). Impairment by suspended solids invasion: testing and prediction. *SPE Production & Facilities, 8*(03), 178-184. [CrossRef]

[17] Eylander, J. G. R. (1988). Suspended solids specifications for water injection from coreflood tests. *SPE Reservoir Engineering, 3*(04), 1287-1294. [CrossRef]

[18] Wojtanowicz, A. K., Krilov, Z., & Langlinais, J. P. (1987, March). Study on the effect of pore blocking mechanisms on formation damage. In *SPE Oklahoma City Oil and Gas Symposium/Production and Operations Symposium* (pp. SPE-16233). SPE. [CrossRef]

[19] Rochon, J., Creusot, M. R., Rivet, P., Roque, C., & Renard, M. (1996, February). Water quality for water injection wells. In *SPE International Conference and Exhibition on Formation Damage Control* (pp. SPE-31122). SPE. [CrossRef]

[20] Pang, S., & Sharma, M. M. (1997). A model for predicting injectivity decline in water-injection wells. *SPE Formation Evaluation, 12*(03), 194-201. [CrossRef]

[21] Sharma, M. M., Pang, S., Wennberg, K. E., & Morgenthaler, L. (1997, June). Injectivity decline in water injection wells: An offshore Gulf of Mexico case study. In *SPE European Formation Damage Conference and Exhibition* (pp. SPE-38180). SPE. [CrossRef]

[22] Bansal, K. M., & Caudle, D. D. (1992, October). A new approach for injection water quality. In *SPE Annual Technical Conference and Exhibition* (pp. SPE-24803). SPE. [CrossRef]

[23] Bennion, D. B., Thomas, F. B., Bennion, D. W., & Bietz, R. F. (1995, June). Mechanisms of formation damage and permeability impairment associated with the drilling, completion and production of low API gravity oil reservoirs. In *SPE International Thermal Operations and Heavy Oil Symposium* (pp. SPE-30320). SPE. [CrossRef]

[24] Al-Taq, A. A., Al-Dahlan, M. N., & Alrustum, A. A. (2017, March). Maintaining Injectivity of Disposal Wells: From Water Quality to Formation Permeability. In *SPE Middle East Oil and Gas Show and Conference* (p. D031S025R004). SPE. [CrossRef]

[25] Karazincir, O., Gomez-Nava, S., Evans, P., Wu, R., Williams, W., Jones, C., & Rijken, P. (2019, September). Impact of Injection Water Quality on Injectivity–A Lab Study. In *SPE Annual Technical Conference and Exhibition* (p. D031S048R004). SPE. [CrossRef]

[26] WANG, X. L. (2008). Current situation and measures of water injection in Chang 8 Layer, Xifeng Oilfield, Changqing Oilfield. *Petroleum Exploration and Development, 35*(3), 344-348. [CrossRef]

[27] Dong, B., Xu, Y., Deng, H., Luo, F., & Jiang, S. (2013). Effects of pipeline corrosion on the injection water quality of low permeability in oilfield. *Desalination, 326*, 141-147. [CrossRef]

[28] Wang, S., Yang, X., Lu, Y., Su, P., Liu, D., Meng, L., ... & Radwan, A. E. (2022). Densification mechanism of deep low-permeability sandstone reservoir in deltaic depositional setting and its implications for resource development: A case study of the Paleogene reservoirs in Gaoshangpu area of Nanpu sag, China. *Frontiers in Earth Science, 10*, 996167. [CrossRef]

[29] National Energy Administration of China. (2022). Water quality technical requirements and analysis methods for water injection in clastic reservoirs (SY/T 5329-2022). Beijing, China: National Energy Administration. Retrieved from https://std.samr.gov.cn/hb/search/stdHBDetailed?id=F38A2BA0F97FF336E05397BE0A0AB6AA

[30] National Energy Administration of China. (2025). Analytical methods for oilfield water (SY/T 5523-2025). Beijing, China: National Energy Administration. Retrieved from https://std.samr.gov.cn/hb/search/stdHBDetailed?id=521363F5E3B289F4E06397BE0A0AFE85